Anhedonia Following Early-Life Adversity Involves Aberrant Interaction of Reward and Anxiety Circuits and Is Reversed by Partial Silencing of Amygdala Corticotropin-Releasing Hormone Gene

Supplemental Information

Supplemental Methods

Chronic early-life stress (CES)

On P2, pups from several litters were gathered, and 12 pups (6 males) were assigned at random to each dam, to prevent the potential confounding effects of genetic variables and litter size. On P2, dams and pups randomly assigned to the CES group were transferred to a cage fitted with a plastic-coated aluminum mesh platform sitting ~2.5 cm above the cage floor. Bedding was reduced to only sparsely cover the cage floor, and one-half of a paper towel was provided for nesting material. Control dams and pups were placed in standard cages, containing a normal amount of bedding (~0.33 cubic feet of corn cob) and one full paper towel. Control (CTL) and CES cages remained undisturbed during P2-P9, during which maternal behaviors were monitored as previously described (1). The CES paradigm provokes significant chronic stress in the pups, as measured by increased corticosterone levels and adrenal hyperplasia, which return to normal by adulthood (2). The stress likely arises because of an abnormal, fragmented pattern of maternal behaviors provoked by the limited nesting material (3, 4). At P21, male rats were weaned and housed 2-3 per cage in a separate animal room of the same facility.

Assessment of anhedonia- and depressive-like behaviors

Sucrose consumption: The test consisted of two phases: one week of habituation, followed by two weeks of sucrose consumption. The first phase allowed the rats to habituate to *ad libitum* access to two bottles containing 50 mL tap water each. In the second phase, one of the bottles

was switched to contain 50 mL of 1.5% sucrose. The left/right position of the bottles was counterbalanced to obviate a side-bias. We measured fluid consumption each morning, and refreshed each drinking solution to 50 mL.

Social play test: The test consisted of three sessions separated by 24 hours. We assessed social interaction behaviors in an open field box (43 x 43 cm) placed in a dimly lit room. The habituation sessions (days 1 and 2) lasted 10 min each. Rats were placed in one corner of an open field and were allowed to explore the box. The apparatus was cleaned with 70% ethanol after each trial. During the testing session on day 3, rats were returned to the testing room, placed in the experimental apparatus and a younger test partner (~P21; to avoid aggressive behaviors) was placed in the box at the opposite corner. Behaviors during a 10-min epoch were monitored using a video camera. The duration of the following behavioral patterns was observed and scored: Following/chasing; kicking (using hind-legs); boxing (pawing upright); wrestling (rolling over one another in rough-and-tumble play); pinning; pouncing (attempting to nose or rub the nape of the neck); sniffing/licking; crawling/climbing. These behavioral patterns were divided into those related to play (following/chasing, kicking, boxing, wrestling, pinning, and pouncing) and behaviors unrelated to play (crawling/climbing and sniffing/licking). No aggressive behaviors were noted.

Forced swim test: The test consisted of two sessions separated by 24 hours. The habituation session (Day 1) lasted 15 min. Rats were placed in a glass cylinder (20 cm in diameter and 60 cm high) containing water (23-25ºC) filled to a depth of 45 cm. The test session occurred 24 hours later, and rats were placed in the cylinder for 5 min. Behavior was monitored using a video camera. The duration of immobility was scored and served as an indicator of depressive-like behaviors. Water was replaced and containers cleaned between trials.

Structural circuitry assessments using magnetic resonance imaging (MRI)

Acquisition: We used an ultra high-resolution MRI scanner (9.4T) with long acquisition times to enhance signal to noise in post-mortem brains. Two cohorts of CTL and CES rats (n=8-9/group; 8 weeks of age) were sacrificed via transcardiac perfusion using 4% paraformaldehyde (PFA). After fixation the brains were removed from the cranial vault and postfixed in 4% PFA, washed and stored at 4°C in 0.1M PB/0.05% azide until DTI. High-resolution T2-weighted (T2WI) and DTI-MR images were acquired using a 9.4T Bruker Biospin MRI system (Paravision 5.1). Brains were positioned in 5-ml plastic syringes and submerged in Fluorinert (Sigma-Aldrich). Each acquisition consisted of 50 0.5 mm slices, 1.92^2 cm field of view, 128^2 matrix zero-filled to 256^2 at reconstruction. Four-shot echo-planar imaging was used to acquire four averages of DTI images with b=0 (5 images) and b=3000 s/mm^2 (30 images in non-colinear directions); diffusion pulse width=4 ms; interpulse=20 ms; repetition time (TR)=12,500 ms; echo time (TE)=36 ms. The resultant DTI scans yielded an acquired in-plane resolution of 150 µm and a reconstructed resolution of 75 µm/voxel. The 0.5-mm slice thickness was utilized to optimize signal to noise whilst minimizing total scan time (1 hr 56 min). The 10 echo T2WI had the following parameters: TR/TE=6500/10 ms and 4 averages with all other parameters being the same.

Structural connectivity analysis: T2 parametric maps were generated using in house MATLAB routines. All DTI and tractography analysis was performed using DSI Studio (National Taiwan University, www.dsi-studio.labsolver.org) (5). Fractional anisotropy (FA), axial (AD) and radial diffusivity (RD) parametric maps were generated in advance of analysis. We focused on two primary regions of interest (ROI): the amygdala and the medial prefrontal cortex (mPFC). The amygdala was outlined on a single FA slice (Bregma: -3.30mm) containing the basolateral and central nuclei, and the mPFC, which was comprised of the cingulate, prelimbic, and infralimbic cortex, was delineated on a FA slice with a Bregma level of 2.70mm. Deterministic tractography was then performed with the following global parameters: seeds=10,000,000 (whole brain);

angular threshold=75, step size=0.05 mm; smoothing=0.60. The fiber threshold varied by subject and was automatically determined by DSI Studio to maximize the variance between the background and foreground. Analysis included tracts (i.e., streamlines) within each hemisphere and those tracts crossing to the adjacent hemisphere. For hemispheric analysis, we circumscribed the tracts using a region of avoidance (ROA) that encompassed the entire adjacent hemisphere.

c-Fos immunocytochemistry

Briefly, after washing (3 x 5 min) with 0.01 M PBS containing 0.3% Triton X-100 (PBS-T; pH=7.4), sections were treated in 0.3% H_2O_2 in 0.01 M PBS for 20 min, followed by blocking of non-specific sites with 1% bovine serum albumin and 2% normal goat serum. Sections were then incubated overnight at room temperature with rabbit anti-c-Fos antiserum (1:10,000; EMD Millipore) in PBS containing 1% bovine serum albumin and 2% normal goat serum, and washed in PBS-T. Sections were incubated in biotinylated goat anti-rabbit IgG (1:400; Vector Laboratories) in PBS-T for 2 h at room temperature. After washing, sections were incubated in the avidin-biotin-peroxidase complex (ABC) solution (1:100; Vector Laboratories) for 3 h and rinsed (3 x 5 min PBS-T), and the reaction product was visualized by incubating the sections in nickel 0.04% 3,3'-diaminobenzidine (DAB) containing 0.01% H_2O_2. This yielded a purple-black nuclear reaction product. Sections were mounted on gelatin-coated slides and coverslipped with Permount (Fisher Scientific).

The Fos-immunoreactive products were analyzed using known landmarks in conjunction with Nissl staining of adjacent sections in series. Fos-positive cells in the central nucleus of amygdala (ACe), basolateral amygdala (BLA), and medial amygdala (MeA) were counted per 10X field per section, corresponding to sections 18-21 (6).

c-Fos and CRF dual-label immunocytochemistry

Following Fos immunocytochemistry (see above), sections were treated in 0.3% H_2O_2 in 0.01 M PBS-T for 20 min, followed by 4% paraformaldehyde for 15 minutes and then rinsed (3 x 5 min PBS-T). Sections were then blocked for non-specific sites with 1% bovine serum albumin and 2% normal goat serum in PBS-T for 30 min, then incubated for 2 days at 4ºC with rabbit anti-CRF antiserum (1:80,000; a gift from Dr. W.W. Vale, Salk Institute) in PBS-T containing 1% bovine serum albumin and 2% normal goat serum, and washed in PBS-T. Sections were incubated in biotinylated goat anti-rabbit IgG (1:400; Vector Laboratories) in PBS-T for 2 h at room temperature. After washing, sections were incubated in the avidin-biotin-peroxidase complex (ABC) solution (1:100; Vector Laboratories) for 3 h and rinsed (3 x 5 min PBS-T). CRF-immunoreactivity, confined to the cytoplasm, was visualized by incubating the sections in 0.04% 3,3'-diaminobenzidine (DAB) containing 0.01% H_2O_2, yielding a homogeneous brown reaction product easily distinguishable from the black nuclear deposit generated by Fos. Sections were mounted on gelatin-coated slides and coverslipped with Permount (Fisher Scientific).

The Fos- and CRF-immunoreactive products were analyzed using known landmarks in conjunction with Nissl staining of adjacent sections in series corresponding to sections 18-21 of the Paxinos rat brain atlas (6). Fos-positive, CRF-positive and dual-positive cells in the central nucleus of amygdala (ACe) were counted per 20X field. Because the distribution of CRF is not homogenous throughout the amygdala, we focused on anatomically matched regions rich in CRF-producing fibers and included two matched sections per rat in the analysis. A similar procedure was used for Fos and Parvalbumin dual-label immunocytochemistry in the medial prefrontal cortex (see below). In all measurements, stereological principles were used to avoid over- or under-sampling (7), and all analyses were performed without knowledge of treatment group.

c-Fos and Parvalbumin dual-label immunocytochemistry

For assessment of Fos, sections were processed as described as above. Once this process was complete, sections were treated in 0.3% H_2O_2 in 0.01 M PBS-T for 20 min, and then blocked for non-specific sites with 1% bovine serum albumin and 2% normal goat serum in PBS-T for 30 min. Sections were incubated overnight at room temperature with mouse anti-Parvalbumin (PV) antiserum (1:50,000; Sigma-Aldrich) in PBS-T containing 1% bovine serum albumin, and then washed in PBS-T. Sections were incubated in biotinylated goat anti-mouse IgG (1:400; Vector Laboratories) in PBS-T containing 1% bovine serum albumin for 3 h at room temperature. After washing, sections were incubated in the avidin-biotin-peroxidase complex (ABC) solution (1:100; Vector Laboratories) for 3 h and rinsed (3 x 5 min PBS-T). PV-immunoreactivity, confined to the cytoplasm, was visualized by incubating the sections in 0.04% 3,3'-diaminobenzidine (DAB) containing 0.01% H_2O_2, yielding a homogeneous brown reaction product easily distinguishable from the black nuclear deposit generated by Fos. Sections were mounted on gelatin-coated slides and coverslipped with Permount (Fisher Scientific).

The Fos- and PV-immunoreactive products were analyzed using known landmarks in series corresponding to sections 9-10 of the Paxinos rat brain atlas (6). Fos-positive, PV-positive and dual-positive cells in the infralimbic prefrontal cortex (IL) were counted per 20X field in anatomically matched sections (4-6 per rat). In all measurements, stereological principles were used to avoid over- or under-sampling (7), and all analyses were performed without knowledge of treatment group.

Analyses and statistical considerations

For c-Fos quantification following social play, an experiment involving two groups (CES and CTL), the mean number of c-Fos positive cells in the ACe were assessed per animal in each group. For sections dually labelled with Fos and CRF, the percentage of dual-labelled cells over total number of c-Fos positive cells in ACe were quantified per animal in each group. An

unpaired, two-tailed t-test was performed to compare CES and CTL groups for these analyses, as well as for sucrose preference and DTI connectivity data. For analyzing the consequences of silencing *Crh*, an experiment involving four groups, a two-way analysis of variance (ANOVA) was employed to determine the main effects and interaction of early-life experience and shRNA intervention.

Supplemental Figures

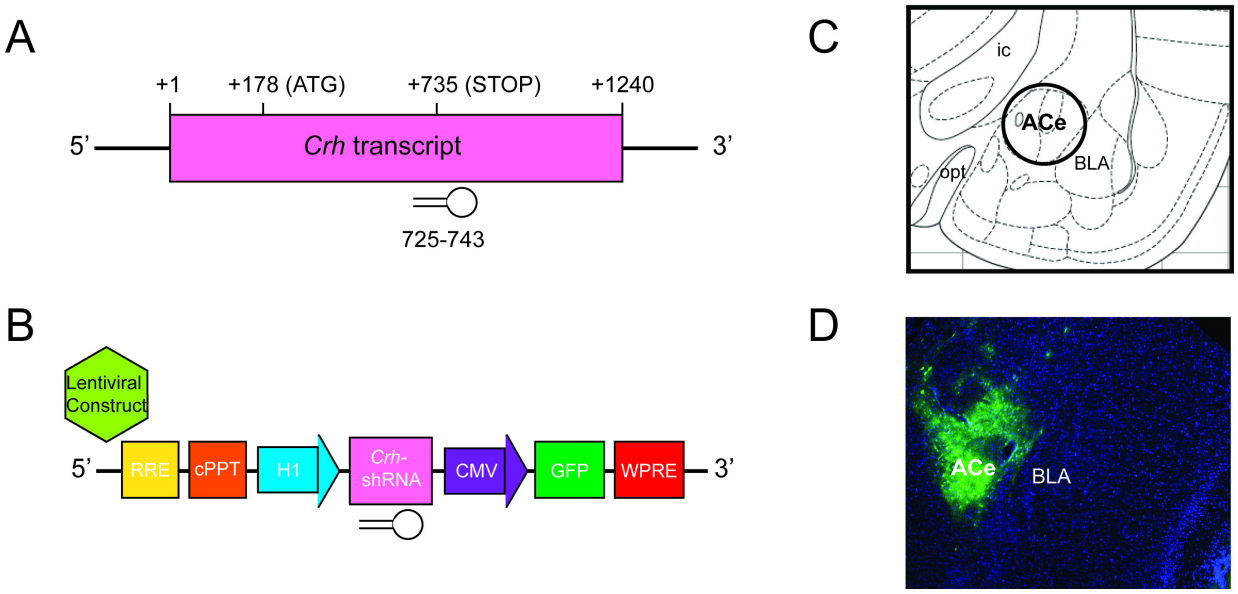

Figure S1. Design and injection of the *Crh*-shRNA-expressing lentiviruses. **(A)** Schematic representation of the shRNA target sequence designed from the open reading frame of the rat *Crh* gene. (**B**) Schematic representation of the lentiviral construct designed to reduce CRF levels and over-express the reporter GFP. This construct has been previously validated *in vitro* and *in vivo* to knockdown *Crh* (8). (**C**) Schematic representation of the region (ACe, circled) where the lentiviral construct was stereotaxically injected into the brain. (**D**) A representative image of the brain of a rat injected with the lentiviral construct. Note that the GFP signifying the presence of construct invades the ACe, but not the neighboring BLA. Brain section was also stained with DAPI, which marks all cell nuclei. *Crh*, corticotropin releasing hormone; GFP, green fluorescent protein; ACe, central amygdala; BLA, basolateral amygdala; DAPI, 4',6-diamidino-2-phenylindole.

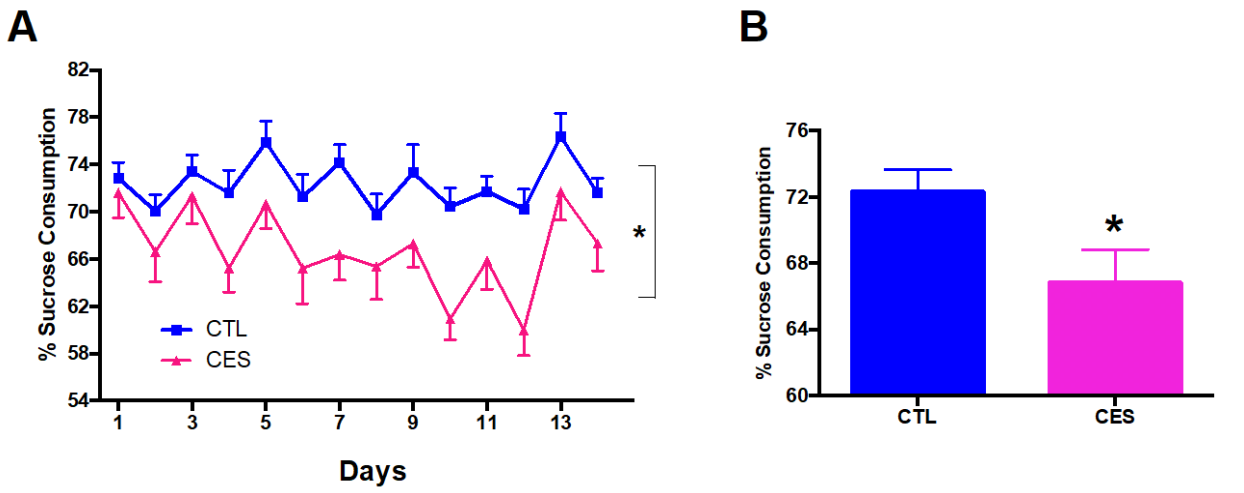

Figure S2. Sucrose preference, a measure of anhedonia, is diminished in CES male adolescent rats. (**A**) Relative consumption of sucrose (% of total fluid intake) was reduced over a 2-week period in rats reared in a CES-promoting environment during P2-9 compared with those reared in routine cages (CTL). (**B**) Data are also presented as the daily average consumption of relative volumes of sucrose. Values are expressed as mean ± SEM (n = 11-12 rats per group; *$p < 0.05$).

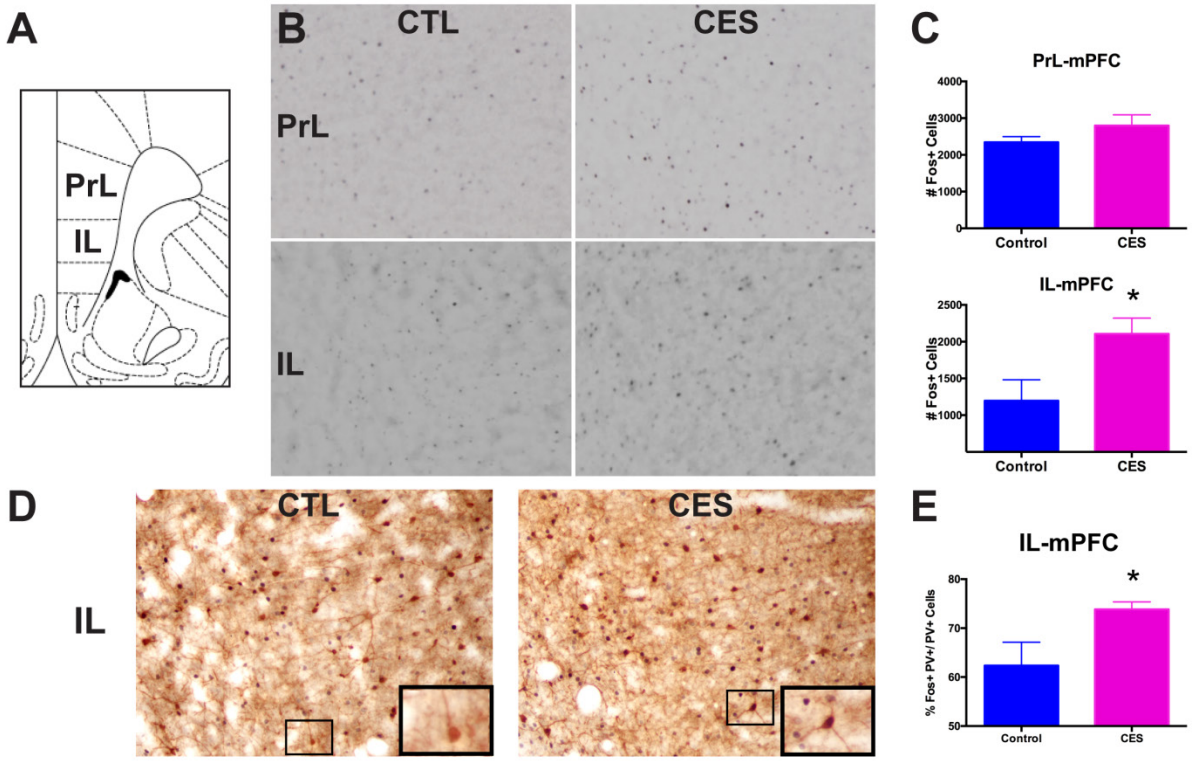

Figure S3. The infralimbic prefrontal cortex (IL) is more activated by social play in CES adolescent rats than in controls. **(A)** Schematic representation of the brain regions where Fos+ cells were counted, including the PrL-mPFC and IL-mPFC. (**B**) Representative images of Fos+ cells in the PrL and IL in CTL and CES adolescent rats sacrificed 90 min. following social play. (**C**) Social play activated a larger number of cells in the IL-mPFC of CES rats compared to controls. (**D**) Representative images of Fos+ (purple-black) and PV+ cells (brown) in the IL-mPFC of CTL and CES adolescent rats sacrificed 90 min. following social play. Insets display a PV+ cell that lacks Fos in a CTL rat (*left*), and a Fos+PV+ (dual-labelled) cell in a CES rat (*right*). (**E**) Of the total number of interneurons in the IL-mPFC (which did not differ in CES vs. CTL), more were identified to be activated by social play (% Fos+ PV+ / PV+) in CES adolescent rats compared to CTL. Values are expressed as mean ± SEM (n = 5 rats per group; *$p < 0.05$).

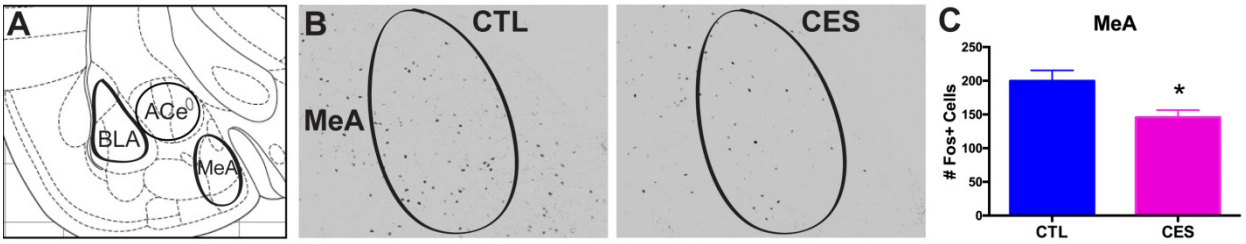

Figure S4. The medial nucleus of the amygdala (MeA) is less activated during social play in CES adolescent rats. (**A**) Schematic representation of the brain regions where Fos+ cells were counted, including the MeA. (**B**) Representative images of Fos+ cells in the MeA in CTL and CES adolescent rats sacrificed 90 min. following social play. (**C**) Social play activated a smaller number of cells in the MeA of CES rats compared to controls. Values are expressed as mean ± SEM (n = 4-5 rats per group; *p < 0.05).

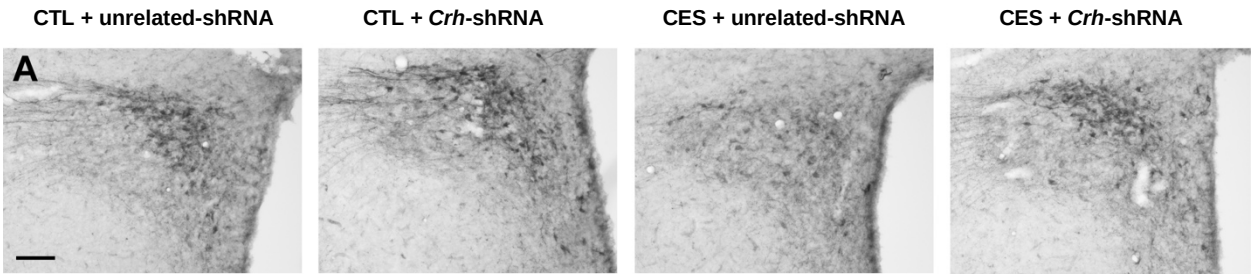

Figure S5. Administration of lentiviral *Crh*-shRNA to ACe did not reduce CRF levels in the hypothalamus. (**A**) Representative images from each group of CRF-immunoreactivity in the PVN of the hypothalamus, an area not targeted by the injection. CRF levels there did not distinguish among groups.

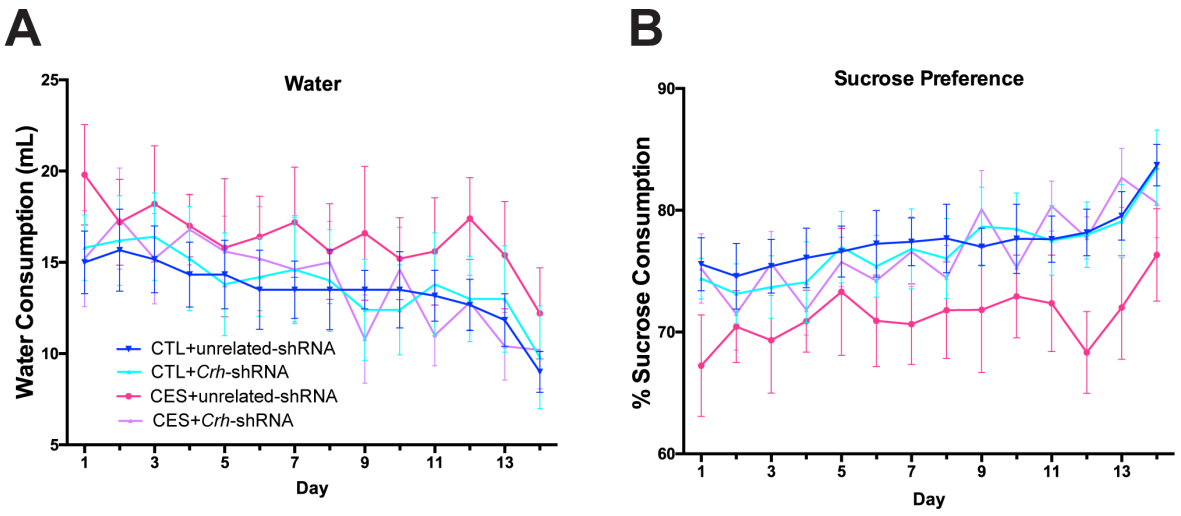

Figure S6. Overall fluid consumption was not influenced by CES or *Crh*-shRNA administration. (**A**) Amount of plain water consumed (mL) over a 2-week period did not distinguish among the groups. (**B**) The % of sucrose consumed trended towards a decrease in CES+unrelated-shRNA rats, but did not reach significance. Values are expressed as mean ± SEM (*n* = 5-6 rats per group).

Supplemental Tables

Table S1. Detailed description of each brain's viral GFP expression. If GFP expression was outside of the ACe (as it was for the majority of brains in the right hemisphere), the presence of CRF-producing cells that could have been impacted by the shRNA is listed in the far right column.

Animal #	Group	Virus Location on Left	Virus Location on Right	CRF+ Cells in Non-ACe Viral Location on Right?
4	CES + *Crh*-shRNA	+ ACe	Intercalated Amygdala (anterior)	No cell bodies
5	CES + *Crh*-shRNA	+ ACe	Caudate Putamen, Internal Capsule	No cell bodies
10	CES + *Crh*-shRNA	+ ACe	Internal Capsule	No cell bodies
18	CES + *Crh*-shRNA	+ ACe	Caudate Putamen	No cell bodies
22	CES + *Crh*-shRNA	+ ACe	+ ACe, Internal Capsule	No cell bodies
2	CTL + *Crh*-shRNA	+ ACe	+ACe, Internal Capsule	No cell bodies
9	CTL + *Crh*-shRNA	+ ACe	Caudate Putamen	No cell bodies
13	CTL + *Crh*-shRNA	+ ACe	+ ACe	
19	CTL + *Crh*-shRNA	+ ACe	+ ACe	
21	CTL + *Crh*-shRNA	+ ACe	+ ACe	
6	CES + unrelated-shRNA	+ ACe	Internal Capsule	No cell bodies
11	CES + unrelated-shRNA	+ ACe	+ ACe, Caudate Putamen	No cell bodies
12	CES + unrelated-shRNA	+ ACe	+ ACe, Caudate Putamen	No cell bodies
16	CES + unrelated-shRNA	+ ACe	+ ACe, Caudate Putamen	No cell bodies
23	CES + unrelated-shRNA	+ ACe	+ ACe, Caudate Putamen	No cell bodies
1	CTL + unrelated-shRNA	+ ACe	+ ACe, Caudate Putamen	No cell bodies
3	CTL + unrelated-shRNA	+ ACe	+ ACe, Caudate Putamen	No cell bodies
8	CTL + unrelated-shRNA		Internal Capsule	No cell bodies
14	CTL + unrelated-shRNA	+ ACe	+ ACe	
15	CTL + unrelated-shRNA	+ ACe	+ ACe, Internal Capsule	No cell bodies
20	CTL + unrelated-shRNA	+ ACe	+ ACe	

Table S2. Number of Fos+ cells in each brain region counted, including reward- and stress-related regions, of adolescent male rats that experienced social play 90-min. prior to sacrifice. Values are mean ± SEM (*n* = 4-5 rats per group; **p* < 0.05).

Brain Region	CTL	CES
Nucleus Accumbens		
Core	453.5 ± 23.9	476.1 ± 75.0
Shell	709.5 ± 65.5	868.7 ± 99.0
Ventral Tegmental Area	421.2 ± 32.8	469.9 ± 27.6
Prefrontal Cortex		
Infralimbic	1195.0 ± 286.0	2106.0 ± 214.7*
Prelimbic	2344.0 ± 153.3	2798.0 ± 292.9
Orbitofrontal	3586 ± 615.5	3638.0 ± 634.5
Habenula		
Medial	8.6 ± 2.0	10.1 ± 4.8
Lateral	41.3 ± 5.8	36.9 ± 5.4
Amygdala		
Central	58.1 ± 9.9	86.9 ± 9.7*
Basolateral	44.5 ± 6.0	43.8 ± 2.3
Medial	199.8 ± 15.8	145.8 ± 10.8*

Supplemental References

1. Ivy AS, Brunson KL, Sandman C, Baram TZ (2008): Dysfunctional nurturing behavior in rat dams with limited access to nesting material: A clinically relevant model for early-life stress. *Neuroscience*. 154: 1132–1142.

2. Brunson KL, Kramár E, Lin B, Chen Y, Colgin LL, Yanagihara TK, *et al.* (2005): Mechanisms of late-onset cognitive decline after early-life stress. 25: 9328–9338.

3. Molet J, Maras PM, Avishai-Eliner S, Baram TZ (2014): Naturalistic rodent models of chronic early-life stress. *Dev Psychobiol*. 56: 1675–1688.

4. Molet J, Heins K, Zhuo X, Mei YT, Regev L, Baram TZ, Stern H (2016): Fragmentation and high entropy of neonatal experience predict adolescent emotional outcome. *Transl Psychiatry*. 6: e702.

5. Yeh F-C, Verstynen TD, Wang Y, Fernández-Miranda JC, Tseng W-YI (2013): Deterministic Diffusion Fiber Tracking Improved by Quantitative Anisotropy. (W. Zhan, editor) *PLoS One*. 8: e80713.

6. Paxinos G, Watson C (1986): *The rat brain atlas*. San Diego, CA: Academic Press.

7. West MJ (1999): Stereological methods for estimating the total number of neurons and synapses: issues of precision and bias. *Trends Neurosci*. 22: 51–61.

8. Regev L, Tsoory M, Gil S, Chen A (2012): Site-Specific Genetic Manipulation of Amygdala Corticotropin-Releasing Factor Reveals Its Imperative Role in Mediating Behavioral Response to Challenge. *Biol Psychiatry*. 71: 317–326.